Biochimica et Biophysica Acta 1798 (2010) 442–452

Contents lists available at ScienceDirect

Biochimica et Biophysica Acta

journal homepage: www.elsevier.com/locate/bbamem

Oxidatively modified fatty acyl chain determines physicochemical properties of aggregates of oxidized phospholipids

Abhay H. Pande *, Subhabrata Kar, Rajan K. Tripathy

Department of Biotechnology, National Institute of Pharmaceutical Education and Research (NIPER), Sector 67, S.A.S. Nagar (Mohali)-160062, Punjab, India

ARTICLE INFO

Article history:
Received 29 July 2009
Received in revised form 14 December 2009
Accepted 29 December 2009
Available online 7 January 2010

Keywords:
Critical micelle concentration
Microfluidity
Micropolarity
Anisotropy
Generalized polarization
Stokes diameter
Surface potential

ABSTRACT

In vivo oxidation of glycerophospholipid generates a variety of products including truncated oxidized phospholipids (tOx-PLs). The fatty acyl chains at the *sn*-2 position of tOx-PLs are shorter in length than the parent non-oxidized phospholipids and contain a polar functional group(s) at the end. The effect of oxidatively modified *sn*-2 fatty acyl chain on the physicochemical properties of tOx-PLs aggregates has not been addressed in detail, although there are few reports that modified fatty acyl chain primarily determines the biological activities of tOx-PLs. In this study we have compared the properties of four closely related tOx-PLs which differ only in the type of modified fatty acyl chain present at the *sn*-2 position: 1-palmitoyl-2-azelaoyl-*sn*-glycero-3-phosphocholine (PazePC), 1-palmitoyl-2-(9′-oxo-nonanoyl)-*sn*-glycero-3-phosphocholine (PoxnoPC), 1-palmitoyl-2-glutaroyl-*sn*-glycero-3-phosphocholine (PGPC), and 1-palmitoyl-2-(5′-oxo-valeroyl)-*sn*-glycero-3-phosphocholine (POVPC). Aggregates of individual tOx-PL in aqueous solution were characterized by fluorescence spectroscopy, size exclusion chromatography, native polyacrylamide and agarose gel electrophoresis. The data suggest that aggregates of four closely related tOx-PLs form micelle-like particles of considerably different properties. Our result provides first direct evidence that because of the specific chemical composition of the *sn*-2 fatty acyl chain aggregates of particular tOx-PL possess a distinctive set of physicochemical properties.

1. Introduction

Oxidation of glycerolphospholipids results in the formation of large number of oxidized phospholipid (Ox-PL) products which are involved in a variety of pathological and physiological functions [1–4]. Different types of Ox-PL generated due to oxidation of glycerolphospholipids include tOx-PLs [2–4]. The *sn*-2 acyl chains of tOx-PLs are shorter in length than the parent non-oxidized phospholipids and bear polar functional group(s) at the end. Lipoprotein particles and cellular membranes are enriched in glycerophospholipids that contain polyunsaturated fatty acids (PUFA) which are the major source for Ox-PLs generation. In mammalian glycerophospholipids, saturated fatty acyl chain of either 16 or 18 carbons usually occupies the *sn*-1 position while the *sn*-2 position usually contains long carbon chain PUFA [2]. Thus most of the Ox-PLs are modified at the *sn*-2 position and results in the generation of different types of tOx-PLs depending on the chain length and degree of unsaturation of fatty acyl chain esterified at the *sn*-2 position of the glycerol [2–4]. The presence of tOx-PLs bearing polar functional group in the lipid bilayers of membrane and lipoproteins is believed to alter several important physicochemical properties of the lipid bilayers [2,5,6]. An increased level of Ox-PLs has been linked with the pathogenesis of various diseases [7,8]. Few reports suggest that the biological activities of these tOx-PLs are determined primarily by the type of acyl chain present at the *sn*-2 position [2,8]. However, the effect of oxidatively modified fatty acyl chain at the *sn*-2 position on the physicochemical properties of tOx-PLs has not been characterized in detail.

Aggregates of lipids are characterized by various methods. Fluorescence spectroscopy has been routinely used to characterize physicochemical properties of aggregates. Because of the instantaneous response of fluorescent parameters of probes to the physicochemical properties of its microenvironment in the aggregates and no major perturbing effect of the fluorescent probes on the aggregates make fluorescence spectroscopy a versatile technique particularly suited for the characterization of physicochemical properties of aggregates [9]. Similarly, size exclusion chromatography (SEC) and native polyacrylamide gel ectrophoresis (PAGE) and agarose gel electrophoresis are powerful techniques that can be used to determine not only the size and homogeneity of the lipid and lipoprotein aggregates but can also be used to characterize the structural features and surface properties of lipid aggregates [10–15].

Abbreviations: ANS, 8-anilinonaphthalene-1-sulfonate; CMC, critical micellar concentration; DPH, 1,6-diphenyl-1,3,5-hexatriene; Laurdan, 2-dimethylamino-(6-lauroyl)-naphthalene; NBD-DMPG, 7-nitrobenz-2-oxa-1,3-diazol-4-yl labeled DMPG; PazePC, 1-palmitoyl-2-azelaoyl-*sn*-glycero-3-phosphocholine; PoxnoPC, 1-palmitoyl-2-(9′-oxo-nonanoyl)-*sn*-glycero-3-phosphocholine; PGPC, 1-palmitoyl-2-glutaroyl-*sn*-glycero-3-phosphocholine; POVPC, 1-palmitoyl-2-(5′-oxo-valeroyl)-*sn*-glycero-3-phosphocholine; tOx-PLs, oxidized phospholipids

* Corresponding author. Tel.: +91 172 2214 682; fax: +91 172 2214 692.
E-mail address: apande@niper.ac.in (A.H. Pande).

0005-2736/$ – see front matter © 2010 Elsevier B.V. All rights reserved.
doi:10.1016/j.bbamem.2009.12.028

In this study we employed fluorescent spectroscopy, size exclusion chromatography and native PAGE and agarose gel electrophoresis to characterize the physicochemical properties of aggregates of four closely related tOx-PLs which differ only in the type of oxidatively modified fatty acyl chain esterified at the *sn*-2 position: PazePC, PoxnoPC, PGPC, and POVPC (Fig. 1). Oxidation of 1-palmitoyl-2-arachidonolyl-*sn*-glycero-3-phosphocholine (PAPC) is known to generate POVPC and PGPC while PazePC and PoxnoPC are formed from the oxidation of 1-palmitoyl-2-linoleoyl-*sn*-glycero-3-phosphocholine (PLPC) [2]. These truncated tOx-PLs are generated in abundance *in vivo* from the action of free radicals or oxidative enzymes on PUFA containing glycerophospholipids in membranes and lipoproteins (reviewed in [1–4]). Our results clearly show that the physicochemical properties of aggregates of closely related tOx-PLs differ widely and depend on the chemical compositions of the oxidatively modified fatty acyl chain present at the *sn*-2 positions of tOx-PL.

2. Materials and methods

2.1. Materials

All lipids including tOx-PLs, NBD-DMPG and C18-PAF were purchased from Avanti Polar Lipids (Alabaster, AL). 8-anilinonaphthalene-1-sulphonic acid (ANS), 1, 6-diphenylhexatriene (DPH), 9-diethylamino-5H-benzo[α] phenoxazine-5-one (Nile Red, NR), acetone, acetonitrile, agarose, blue dextran, chloroform, ethanol, EDTA, dimethyl formamide (DMF), methanol, 1-propanol, 1-butanol, sodium dodecyl sulphate (SDS), Sepharose 4B, tryptophan, and tetrahydrofuran were purchased from Sigma-Aldrich (Bangalore, India). Laurdan (2-dimethylamino-(6-lauroyl)-naphthalene) was obtained from Molecular Probes (Eugene, OR, USA). Pre-casted tris–glycine gel (4–20%), tris–glycine native running buffer, tris–glycine native sample buffer and NativeMark unstained protein standards were purchased from Invitrogen (Bangalore, India). All other reagents used were of analytical grade. Buffer used was prepared in double distilled deionized water.

2.2. Sample preparation

Stock solutions of the fluorescent dyes were made in the following solvents: ANS and Nile Red in acetone, Laurdan in ethanol, and DPH in DMF. To prepare stock tOx-PLs solutions in aqueous buffer, 100 µl of lipid stock solutions in chloroform (8 mM) was taken and the solvent was removed under nitrogen, followed by desiccation for ~3 h under vacuum. The dry lipid film was then hydrated by adding 200 µl of aqueous buffer containing 10 mM Hepes, 10 mM NaCl, 1 mM EDTA (pH 7.4) and vortexing the tubes at room temperature. NBD-DMPG (0.05 mol%) labeled tOx-PLs were prepared by adding an appropriate amount of NBD-DMPG from the stock to tOx-PL followed by the removal of solvent under nitrogen, desiccation under vacuum and finally rehydration of dry film at room temperature by adding an aqueous buffer as described above.

2.3. Fluorescence measurements

All fluorescence measurements were carried out on a Shimadzu Spectrofluorophotometer RF-5301PC (Shimadzu, Kyoto, Japan) using 4×4 mm quartz cuvette (Perkin-Elmer (India) Pvt. Ltd., India). The temperature was adjusted to 25 ± 0.5 °C by a constant temperature water circulator (NTT-2200P) and the sample in the cuvette was stirred constantly with the stirrer. Excitation and emission slits were 5 and 10 nm, respectively. In all experiments the composition of the buffer used was 10 mM Hepes, 10 mM NaCl, and 1 mM EDTA (pH 7.4). All spectra were corrected by subtracting the spectra of buffer, smoothed (Savitzky–Golay, 11 points) and emission intensity at particular wavelength was determined.

The critical micelle concentrations (CMC) of tOx-PLs were determined by linear least-squares fitting of the fluorescence emission data as the function of tOx-PL concentrations before and after the change of slope. The CMC was calculated at the intersection of these lines as [16]:

$$-CMC = A / B \quad (1)$$

where, A is the intercept difference and B is the slope difference.

2.4. Fluorescence measurements using ANS as a probe

To a 0.5 ml solution of 7.5 µM ANS in aqueous buffer, small aliquots of tOx-PL were added from the aqueous stock solutions with continuous stirring. Two minutes after each addition fluorescence emission spectra of the ANS were recorded from 370 nm to 570 nm using an excitation wavelength of 356 nm. To determine the CMC of tOx-PL, change in the fluorescence emission maxima, $(\Delta\lambda_{max} = \lambda_{max \text{ in absence of Ox-PL}} - \lambda_{max \text{ in presence of Ox-PL}})$ was plotted as a function of tOx-PL concentrations.

2.5. Fluorescent measurements using Laurdan as a probe

Small aliquots of tOx-PL stock solutions in aqueous buffer were added to 0.5 ml of 7.5 µM solution of Laurdan in aqueous buffer with continuous stirring. Fluorescence emission spectra of the Laurdan were recorded from 390 nm to 600 nm by using the excitation wavelength of 360 nm 2 min after each addition. Generalized polarization (GP) for Laurdan was calculated from emission spectra by using following equation [17]:

$$GP = (F_{440} - F_{490}) / (F_{440} + F_{490}) \quad (2)$$

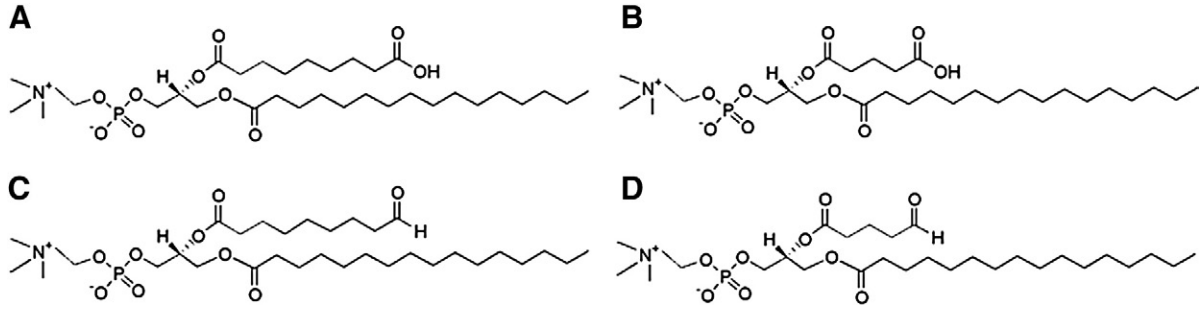

Fig. 1. The structures of the tOx-PLs used in the present study. (A) 1-palmitoyl-2-azelaoyl-*sn*-glycero-3-phosphocholine (PazePC), (B) 1-palmitoyl-2-glutaroyl-*sn*-glycero-3-phosphocholine (PGPC), (C) 1-palmitoyl-2-(9′-oxo-nonanoyl)-*sn*-glycero-3-phosphocholine (PoxnoPC), and (D) 1-palmitoyl-2-(5′-oxo-valeroyl)-*sn*-glycero-3-phosphocholine (POVPC).

where, F_{440} and F_{490} are the fluorescence emission intensities at 440 and 490 nm, respectively.

2.6. Fluorescent measurements using DPH as a probe

To a 0.5 ml solution of 7.5 μM DPH small aliquots of tOx-PL were added from the stock solutions with continuous stirring. Two minutes after each addition fluorescence emission spectra of the DPH were recorded from 390 nm to 490 nm by exciting the DPH at 366 nm. For fluorescence depolarization measurement emission spectra were recorded both when the emission polarizer was parallel and perpendicular to the direction of polarization of the excitation beam in an L-format geometry of detection.

To determine the CMC of tOx-PLs, total fluorescence emission intensity (F_T) at 430 nm was calculated by using the following relationship [18]:

$$F_T = F_{||} + 2F_{\perp} \tag{3}$$

where, $F_{||}$ and $F_{\perp}$ are the fluorescence emission intensities at 430 when the emission polarizer was parallel and perpendicular, respectively, to the direction of polarization of the excitation beam. Total fluorescence emission intensity (F_T) was then plotted as a function of tOx-PL concentrations.

Steady-state fluorescence anisotropy (r) values of DPH were obtained using the expression [18]:

$$r = F_{||} - GF_{\perp} / F_{||} + 2GF_{\perp} \tag{4}$$

where, G is an instrumental correction factor that corrects for unequal transmission by the diffraction gratings of the instrument for vertically and horizontally polarized light [18].

2.7. Fluorescent measurements using Nile Red as a probe

To the 400 μM of particular tOx-PL in aqueous buffer was added 0.1 μM of Nile Red and the emission spectra of the dye were determined from 560 nm to 700 nm by using the excitation wavelength of 549 nm. The fluorescence emission spectra of Nile Red are known to be strongly dependent on the polarity of the medium. To determine the micropolarity around Nile Red in the aggregates of tOx-PLs, the fluorescence emission maxima of Nile Red (0.1 μM final concentration) was measured in solvents of different polarities. After subtracting the spectra of respective sample without dye, the fluorescence emission maximum (λ_{max}) was determined and plotted as a function of relative polarities of the solvents to generate a standard curve. The micropolarity around Nile Red in the aggregates of tOx-PLs was determined from the standard curve [19].

2.8. Size exclusion chromatography of tOx-PLs

Aqueous suspension of tOx-PL was subjected to size exclusion chromatography according to published procedures [11,12,20] with minor modifications. Chromatography was done using AKTApurifier UPC FPLC protein purification system (GE Healthcare Bio-Sciences Ltd., Uppsala, Sweden) and the buffer used was 10 mM Hepes, 10 mM NaCl, 1 mM EDTA, and pH 7.4. One hundred microliter of tOx-PL suspension in aqueous buffer (1.75 mM final concentration) was applied to a Sepharose 4B column (1.5×25 cm) and eluted in the same buffer at a flow rate of 0.2 ml/min buffer. The effluent was monitored at 280 nm wavelength. The total volume (V_t) and void volume (V_o) of the packed column was determined from the elution of tryptophan and blue dextran, respectively.

2.9. Native PAGE of tOx-PLs

For native PAGE analysis NBD-DMPG (0.05 mol%) labeled tOx-PL suspensions (1.75 mM final concentration) were prepared as describe in Section 2.2. Recently it has been shown that a trace amount of NBD-DMPG, used as a fluorescent marker, does not affect the aggregation of lipids and lipoproteins [21]. Equal amounts of aqueous tOx-PL suspension are diluted with 2× native gel sample buffer and loaded onto 4–20% pre-casted tris–glycine gel. Samples were electrophoresed using a miniVE electrophoresis unit (GE Healthcare Bio-Sciences Ltd., Uppsala, Sweden) under conditions of constant voltage. After electrophoresis, lipid aggregates in the gel were directly imaged using Typhoon Trio™ Variable Mode Imager (GE Healthcare Bio-Sciences Ltd., Uppsala, Sweden) using an excitation wavelength of 488 nm (blue laser) and an emission wavelength of 520 nm bandpass 40 filter. The protein bands (molecular weight marker) in the gel were detected by using Bio-Rad Silver Stain Plus kit. The Stokes diameter of the lipid aggregates were determined from a calibration curve generated using the proteins present in the NativeMark protein standards.

2.10. Agarose gel electrophoresis of tOx-PLs

Surface potential of tOx-PL particles were determined by electrophoresis on 0.5% agarose according to the method of Sparks and Phillips [13]. Equal amounts of aqueous tOx-PL suspension of NBD-DMPG (0.05 mol%) labeled tOx-PL suspensions (1.75 mM final concentration) were diluted with 5× loading buffer (0.5% bromophenol blue and 50% glycerol in tris–acetate buffer, pH 8.6) and 10–12 μl of these samples were applied to 10-cm agarose gel. The electrophoresis was performed at constant voltage (180 V) in 50 mM tris–acetate buffer, pH 8.6 for 1 h or until the dye reached the other end. After electrophoresis, lipid aggregates in the gel were directly imaged using Typhoon Trio™ Variable Mode Imager as described in Section 2.9. Surface potential of the lipid aggregates was determined as described previously [13]. Briefly, electrophoretic mobilities (U) of the aggregates were calculated by dividing the electrophoretic velocity (mean migration distance (mm) per time in seconds) by the electrophoretic potential (voltage per gel distance in cm). Correction of the pI-dependent retardation effects was done using the following equation [13]:

$$U_{corrected} = (U_{agarose} - 0.136) / 1.211 \tag{5}$$

The surface potentials of tOx-PL aggregates were calculated by using the following equation:

$$S = U \times 6\pi n / D \tag{6}$$

where n is the coefficient of viscosity (0.0089 poise), and D is the solvent dielectric constant [13].

3. Results

Aggregates of tOx-PL were characterized using fluorescent spectroscopy, size exclusion chromatography and native PAGE and agarose gel electrophoresis. Fluorescent probes used in this study possess different chemical properties that enable them to reside in particular location in the lipid aggregates and report the information of microenvironment from that region of the aggregates. While ANS provides the information of micropolarity at the lipid–water interface of lipid aggregates [22], Laurdan reports the hydration and mobility changes at the level of the *sn*-1 carbonyl group [23]. Similarly, DPH provides the information of microfluidity of the hydrocarbon core of the aggregates [24] and Nile Red reports the micropolarity of the hydrocarbon core of the aggregates of lipids [25].

3.1. Characterization using ANS as a probe

ANS is an amphiphilic, anionic, environmentally sensitive fluorescence probe, which we used to detect the micropolarity of its binding environment as well as to quantitate the CMC of tOx-PLs. ANS is known to be located at the interface between the polar phase and apolar phase (at the surface of lipid aggregates) due to the balance of hydrophobic and hydrophilic interactions [22,26]. The fluorescence yield of ANS is very low in an aqueous environment and the yield increases significantly upon transfer of ANS to a hydrophobic environment [27,28]. The tOx-PLs at different concentrations were mixed with fixed concentration of ANS and the fluorescent emission spectra were recorded. As depicted in Fig. 2 initially increasing concentrations of tOx-PLs resulted in a small increase in the emission intensities of ANS. After the threshold concentrations of tOx-PLs, there was a large increase in the emission intensity of ANS accompanied by the blue shift in the emission maximum. The blue shift of ANS emission maximum in the presence of tOx-PLs indicates that the lipids are in the form of micelles or aggregates in an aqueous solution. The position of the emission maxima can provide information about the 'micropolarity' of the environment around the fluorophore. Careful analysis of the ANS spectra in presence of increasing concentrations of tOx-PLs revealed that the extent of blue shift in the emission maximum is distinct for different lipids. PazePC and PGPC, which contain truncated *sn*-2 acyl chain bearing carboxyl function, exhibited the blue shift of ~13 nm and ~5 nm, respectively. And PoxnoPC and POVPC which contain truncated *sn*-2 acyl chain bearing aldehydic functional group displayed the blue shifts of ~12 nm and ~17 nm, respectively. However, the extent of blue shift in the emission maxima of ANS observed in the presence of aggregates of tOx-PLs used in this study was considerably less compared to the blue shift in the emission maxima when the ANS probe goes in complete hydrophobic (apolar) environments [27,28]. These observations indicate that (a) microenvironment of ANS in the aggregates of PGPC is relatively more polar than POVPC and, (b) the ANS resides at much shallower positions in the aggregated forms of all four tOx-PLs studied here.

The CMC of tOx-PLs was determined by plotting the change in the emission maxima ($\Delta\lambda_{max}$) as a function of Ox-PL concentrations (Fig. 3). Concentration of lipid corresponding to the intersection of the two straight lines fitting the data is taken as the CMC value. The CMC values of four tOx-PLs were found to be in the range of 19.5 to 66.9 μM and were in the following decreasing order: POVPC>PGPC>PoxnoPC>PazePC (Table 1). Under identical experimental conditions, CMC of the SDS, which was used as a control, was found to be 8.51 ± 0.66 mM (see supplementary data 1), which agree well with the published CMC value of SDS [27].

3.2. Characterization using Laurdan as a probe

The fluorescence emission spectrum of Laurdan, an amphiphilic fluorescent probe, is very sensitive to the hydrophobic / hydrophilic character of its surrounding microenvironment. In solvents of high polarity, the emission spectra of Laurdan show a considerable shift to longer wavelengths due to the dipolar relaxation processes [17]. Laurdan incorporated in phospholipid membrane locates itself at the hydrophilic–hydrophobic interface of the bilayers with its lauric acid tail anchored in the phospholipid acyl chains region while its fluorescing moiety is located at the glycerol level of the phospholipid headgroup [23]. Membrane incorporated probe reports the physicochemical properties (e.g. micropolarity and microfluidity changes) at the level of the *sn*-1 carbonyl group in the phospholipids membrane [23].

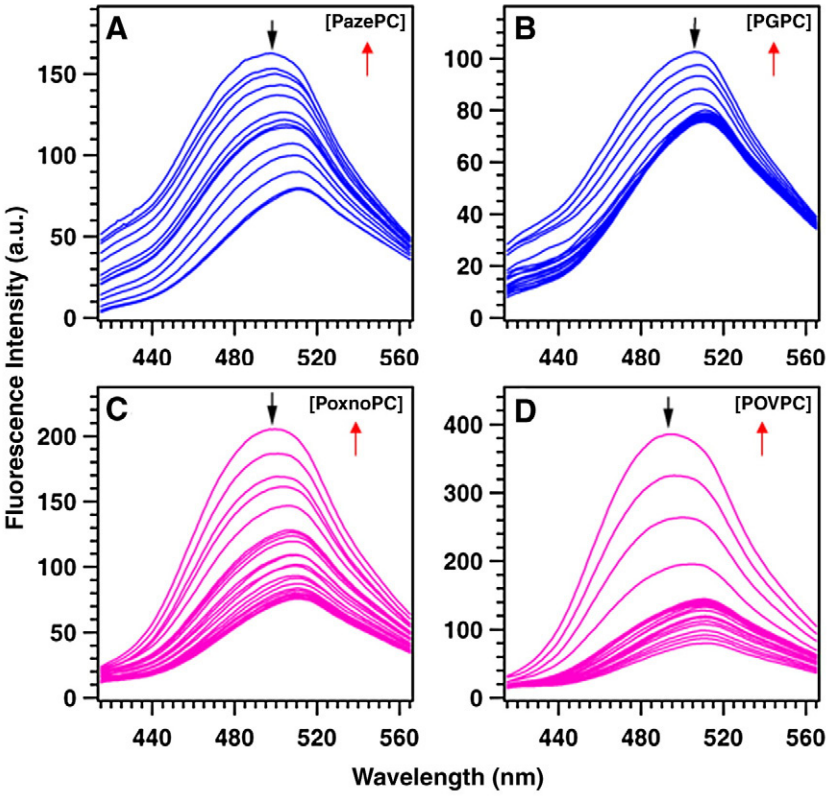

Fig. 2. Fluorescence emission spectra of ANS in the presence of increasing concentrations of (A) PazePC, (B) PGPC, (C) PoxnoPC and (D) POVPC. Increasing concentrations of tOx-PL, indicated by red arrows, were added to a solution of 7.5 μM ANS in a]ueous buffer with continuous stirring. Two minutes after each addition fluorescence emission spectra of the ANS were recorded at 25 °C. The concentrations of tOx-PLs increased were from 0 to 150 μM except for PazePC whose concentration used was 0–82 μM. Black arrows indicate the fluorescence emission maxima (λ_{max}) of ANS in presence of maximum concentration of tOx-PLs.

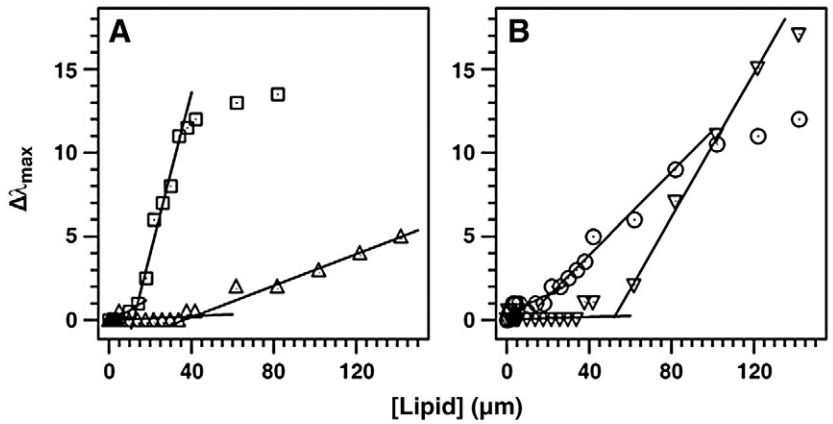

Fig. 3. Change in the fluorescence emission maxima ($\Delta\lambda_{max}$) of ANS as a function of tOx-PL concentrations. Experiments were conducted as describe in the legend of Fig. 2 and emission maximum of each spectrum was determined. Change in the emission maximum of ANS, $\Delta\lambda_{max}$, ($\Delta\lambda_{max} = \lambda_{max\ in\ absence\ of\ Ox\text{-}PL} - \lambda_{max\ in\ presence\ of\ Ox\text{-}PL}$) was calculated and plotted as a function of tOx-PL concentrations. Symbols used in panel A (□; PazePC, Δ; PGPC) and in panel B (○; PoxnoPC, ▽; POVPC).

Fluorescence emission spectra of Laurdan in presence of increasing concentrations of tOx-PLs are shown in Fig. 4. Addition of tOx-PLs resulted in increase in the emission intensity of Laurdan. In the case of PoxnoPC and POVPC when the lipid concentration is low, larger initial increase in the emission intensities were observed which reached to saturation at higher lipid concentrations (Fig. 4C, D) while in the case of PGPC a small increase in emission intensity was observed when the tOx-PL concentration was low and with an increase in lipid concentration (above CMC values) the increase in the intensity was steep and then shows fewer changes at a higher concentration (Fig. 4B). These observations clearly show the difference in the kinetic of aggregates formation by closely related tOx-PLs. Also fluorescence emission spectra of Laurdan in the aggregates of different tOx-PL, i.e. at concentrations above CMC values of tOx-PLs, exhibited distinctive features. PGPC and POVPC which contain 5-carbon *sn*-2 acyl chain bearing polar functional groups exhibited the maximum emission at 487–488 nm while PazePC and PoxnoPC, which contain 9-carbon *sn*-2 acyl chain bearing polar functional groups, revealed asymmetrical emission spectra with a maximum at 473–475 nm and a pronounced shoulder at ~433 nm. These spectral features reflect differences in the properties of aggregates of tOx-PLs [29]. For the same concentration of Laurdan, the increase in emission intensity is relatively higher in tOx-PLs containing aldehydic functional group than lipids containing carboxylic function, suggesting that the former tOx-PLs provides relatively more hydrophobic microenvironment to Laurdan than the latter [30].

The spectral changes in the emission spectrum of Laurdan can be characterized by the generalized polarization value (GP). GP for Laurdan was calculated from emission spectra by using Eq. (2) and plotted as a function of tOx-PL concentrations (Fig. 5). GP values of Laurdan in aggregates of tOx-PLs formed above their CMC were found to be -0.11 ± 0.12, -0.04 ± 0.06, -0.42 ± 0.22, and -0.31 ± 0.20 for PazePC, PoxnoPC, PGPC and POVPC, respectively (Table 1). The GP value of dye in aggregates of SDS, used as a control, above its CMC was found to be -0.86 ± 0.08 (see supplementary data 2). It has been shown that the GP value decreases when the penetration of water molecules into the bilayers increases. The red shift in the Laurdan fluorescence emission spectrum is caused by dipole–dipole interactions and reorientation of water molecules in the vicinity of the Laurdan probe in the aggregates [31]. Our results suggest that the Laurdan, which resides at the level of the *sn*-1 carbonyl group, experience relatively more polar environment in the aggregates of POVPC and PGPC compared to PazePC and PoxnoPC.

Table 1
Critical micellar concentrations (in μM) and physicochemical properties of aggregates of tOx-PLs determined using fluorescent probes.

tOx-PLs	CMC (in μM) determined using		GP of Laurdan in aggregates of tOx-PLs formed above their CMC	Fluorescence anisotropy of DPH in aggregates of tOx-PLs formed above their CMC
	ANS as a probe	DPH as a probe		
PazePC	19.5 ± 9.9	23.1 ± 10.4	−0.11 ± 0.12	0.11 ± 0.01
PoxnoPC	29.3 ± 13.7	34.9 ± 11.1	−0.04 ± 0.06	0.21 ± 0.02
PGPC	54.6 ± 12.5	53.6 ± 9.1	−0.42 ± 0.22	0.04 ± 0.01
POVPC	66.9 ± 14.1	69.4 ± 13.1	−0.31 ± 0.20	0.05 ± 0.03

Each data point represents the average of three independent experiments and is expressed as mean ± SEM.

3.3. Characterization using DPH as a probe

Fluorescent properties of DPH are very sensitive to the process of micellization of various monomers in an aqueous medium [32]. DPH is nonfluorescent in an aqueous medium and shows a remarkable increase in intensity as it goes into the nonaqueous medium. The emissions spectra of DPH in presence of increasing concentrations of tOx-PLs were measured and the representative spectra are presented in Fig. 6A and B. Fluorescence emission spectra when the emission polarizer was parallel and perpendicular, respectively, to the direction of polarization of the excitation beam are shown by continuous and dotted lines, respectively. Initially when the concentrations of tOx-PL are low, the emission intensities of DPH were almost close to zero. As the concentrations of lipid increased the emission intensities showed a steep increase. When the emission polarizer was parallel to the direction of polarization of the excitation beam (continuous pink lines), the emission spectra of DPH exhibit a major peak centered at ~430 nm and a prominent shoulder at ~405 nm. While, the emission spectra exhibit a major peak centered at ~430 nm and a prominent shoulder at ~460 nm when the emission polarizer was perpendicular to the direction of polarization of the excitation beam (dotted blue lines). These features of the emission spectra of DPH in the presence of Ox-PL are typical of those reported for DPH in other lipid aggregated systems [33].

Total emission intensities of DPH in the presence of increasing concentrations of tOx-PLs were calculated using Eq. (3) and plotted as a function of concentrations of tOx-PL (Fig. 6C and D). CMC values for each tOx-PLs were found to be in the range of 23.1 μM to 69.4 μM and were in the decreasing order of POVPC>PGPC>PoxnoPC>PazePC (Table 1). Under identical experimental conditions, the CMC value of the SDS, which was used as a control, was found to be 8.36 ± 1.2 mM (see supplementary data 3).

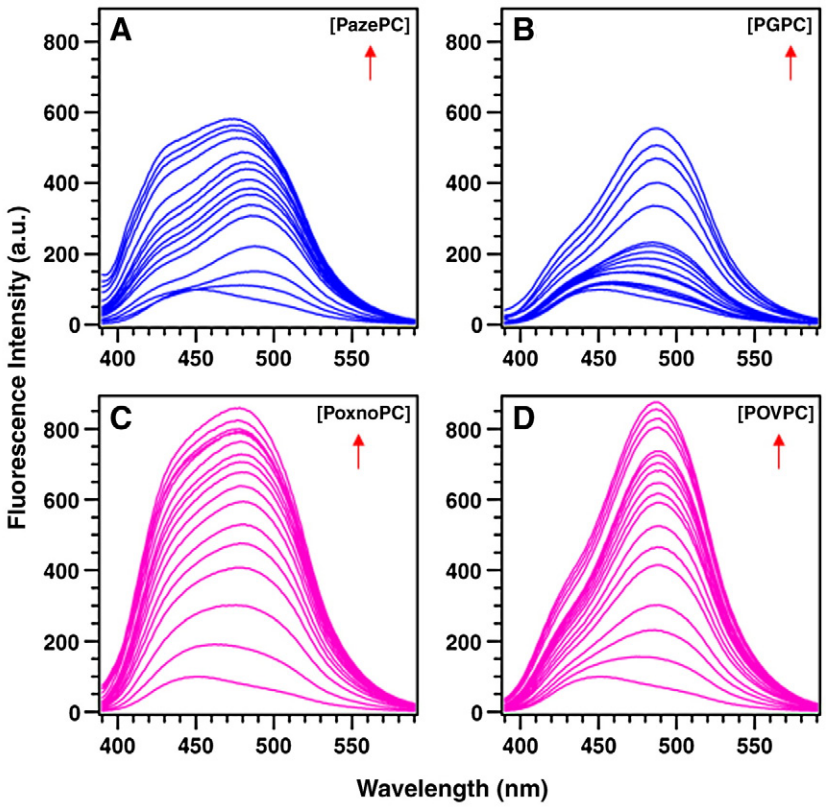

Fig. 4. Fluorescence emission spectra of Laurdan in the presence of increasing concentrations (0–150 μM) of (A) PazePC, (B) PGPC (C) PoxnoPC, and (D) POVPC. To the solution of 7.5 μM Laurdan in aqueous buffer increasing concentrations of tOx-PLs, indicated by red arrows, were added and fluorescence emission spectra were recorded at 25 °C.

Steady-state fluorescence anisotropy (r) of DPH incorporated into the aggregates provides information about the organization of the aggregates microenvironment around the fluorescent probe. The change in the polarization of DPH fluorescence thus acts as an index for the change in microviscosity of the immediate environment i.e. the lipidic core of the aggregates [34]. Steady-state fluorescence anisotropy values of DPH in the presence of increasing concentrations of tOx-PLs were calculated using Eq. (4) and plotted as a function of tOx-PLs concentrations (Fig. 7A and B).When the concentration of lipid was low, the anisotropy was found to be high (~0.12), which can be due to the hydrophobic aggregation of DPH in aqueous medium as the probe is known to be extremely hydrophobic. Increasing concentrations of tOx-PLs resulted in different profiles of anisotropy of DPH (Fig. 7A and B). The values of fluorescence anisotropy of DPH in the aggregates of tOx-PLs formed above their CMC were found to be in the decreasing order of PoxnoPC>PazePC>POVPC≈PGPC (Table 1). These observations suggest that the observed changes in anisotropy of DPH may be due to the different nature of aggregates (spherical micelles, rod-like micelles, vesicles etc. [40]) and/or due to the different chemical compositions of tOx-PLs species used.

3.4. Characterization using Nile Red as a probe

Nile Red is a solvatochromic dye and the spectral position, shape and intensity of its emission spectrum are strongly dependent on the polarity of the solvent [25]. The dye molecule is insoluble in water and

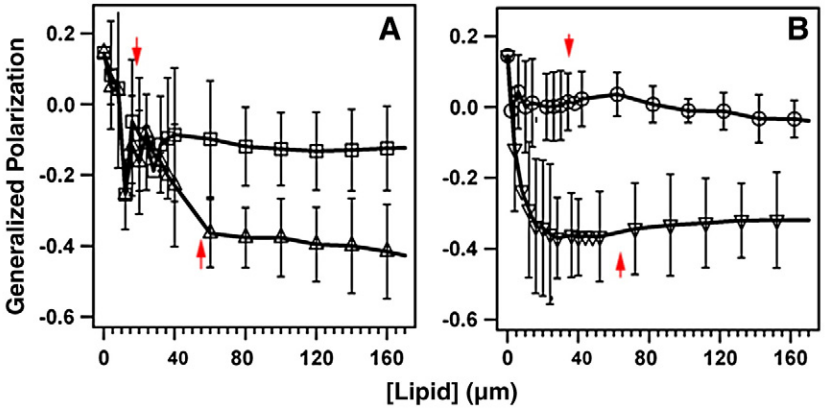

Fig. 5. Dependence of generalized polarization of Laurdan as a function of tOx-PL concentrations. Experiments were conducted as describe in the legend of Fig. 4. Symbols used: (□); PazePC, (Δ); PGPC, (○); PoxnoPC, and (▽) POVPC. Each data point represents the average of three independent experiments and is expressed as mean ± SEM. Red arrows indicate the average CMC of tOx-PL.

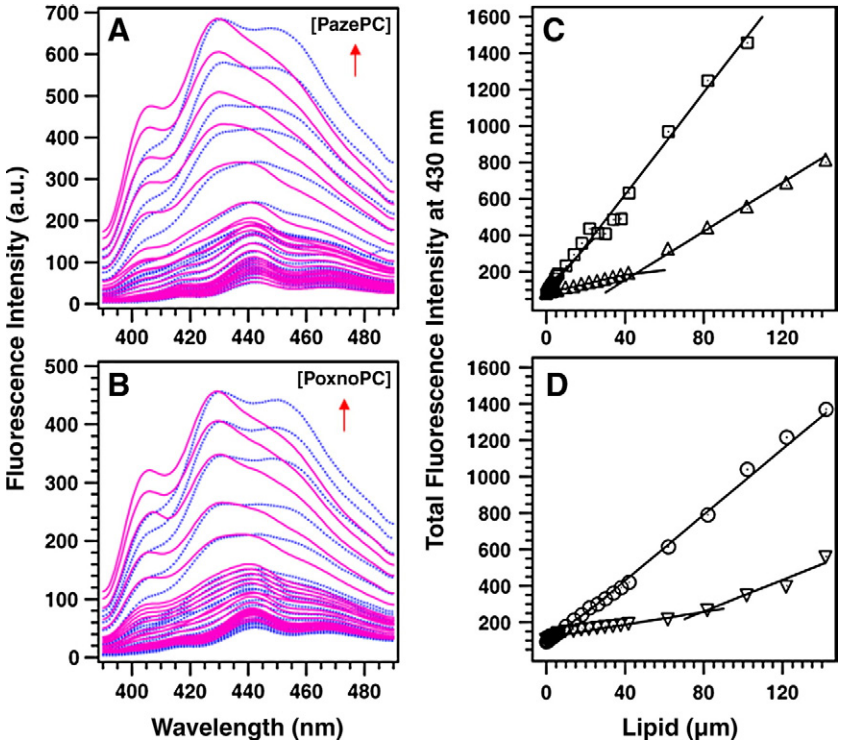

Fig. 6. Fluorescence emission spectra (A and B) of DPH as a function of tOx-PL concentrations. To the sample of 7.5 μM DPH in aqueous buffer increasing concentrations of tOx-PL, indicated by red arrows, were added and fluorescence emission spectra of the DPH were recorded. Representative emission spectra of DPH in presence of increasing concentrations of (A) PazePC and (B) PoxnoPC, recorded when the emission polarizer was parallel (continuous pink lines) and perpendicular (dotted blue lines) to the direction of polarization of the excitation beam are shown. Dependence of total fluorescence emission intensity of DPH as a function of tOx-PL concentration (C and D). Symbols used: (□); PazePC, (Δ); PGPC, (○); PoxnoPC, and (▽) POVPC.

locates itself only into the hydrophobic region in the micelles/aggregates resulting in an intense fluorescence emission [33]. Therefore, it was expected that the emission maximum of Nile Red in the tOx-PL aggregates will provide information on the micropolarity around the hydrocarbon chains. Fluorescence emission spectra of Nile Red in the solvent of differing polarities [51] were recorded and are presented in Fig. 8A. Increase in polarity of solvent decreased the emission intensity and resulted in the red shift in the emission maxima of the probe. Similarly, the emission spectra of Nile Red in presence of 400 μM of tOx-PLs are recorded and presented in Fig. 8B. The intensities, shapes and positions of emission spectra of Nile Red were found to differ in the presence of tOx-PLs. The emission maxima of Nile Red in presence of PoxnoPC, PazePC, POVPC and PGPC were found to be at 616.5, 626.5, 628.0, and 631.0 nm, respectively, which corresponds to the relative polarities of 0.579, 0.700, 0.717, and 0.752, respectively (Fig. 8C). These results indicate that the hydrocarbon region around Nile Red in PGPC and POVPC micelles is more hydrated than PazePC and PoxnoPC.

3.5. Size exclusion chromatography of tOx-PL aggregates

SEC of lipids has been used earlier for purification of phospholipids MLVs and SUVs as well as for the characterization of basic geometric and structural features of lipid vesicles [11,12,20,35]. In order to

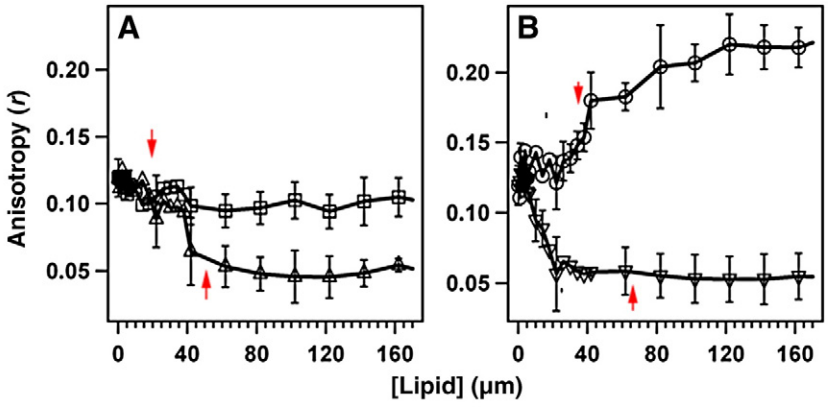

Fig. 7. Steady-state fluorescence anisotropy (r) of DPH as a function of tOx-PL concentrations. Experimental details are given in the legend of Fig. 6. Fluorescence emission intensities at 430 nm were determined when the emission polarizer was parallel and perpendicular to the direction of polarization of the excitation beam and fluorescence anisotropy of DPH was calculated using Eq. (4). Symbols used: (□); PazePC, (Δ); PGPC, (○); PoxnoPC, and (▽) POVPC. Each data point represents the average of three independent experiments and is expressed as mean ± SEM. Red arrows indicates the average CMC of tOx-PL.

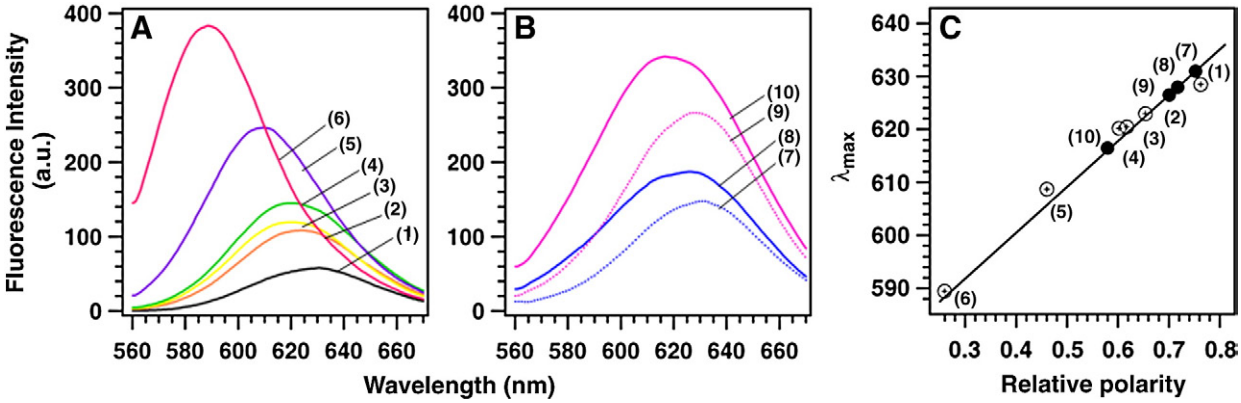

Fig. 8. Fluorescence emission spectra of Nile Red (0.1 μM final concentration) in solvents of different polarities (A) and in presence of 400 μM of tOx-PLs in aqueous buffer (B). Fluorescence emission maximum (λ_{max}) of Nile Red was plotted as a function of relative polarities of the solvents (C).Data was fitted to non-linear regression analysis to get the standard curve and the micropolarity of Nile Red incorporated into the aggregates of tOx-PLs was evaluated using the standard curve. Symbols: (1) methanol, (2) ethanol, (3)1-propanol, (4) 1-butanol, (5) acetonitrile, (6) tetrahydrofuran, (7) PGPC, (8) POVPC, (9) PazePC, and (10) PoxnoPC.

determine the size of aggregates of tOx-PL, gel filtration chromatographic analysis of aqueous suspension to tOx-PL using Sepharose 4B column was carried out. The elution profile of lipids and markers is presented in Fig. 9 as a plot of OD_{280} versus elution volume. The total volume ($V_t = 10.25 \pm 0.07$ ml) and void volume ($V_o = 3.65 \pm 0.04$ ml) of the packed column were determined from the elution of tryptophan and blue dextran, respectively. In Fig. 9, the elution positions of blue dextran and tryptophan are shown by blue and black arrows, respectively. Aqueous suspension of equimolar concentration of POPC and POPG, prepared similarly as tOx-PL suspension and used as a marker of MLVs, was eluted at $V_e = 3.65 \pm 0.08$ ml (dotted brown lines). Elution profile of aqueous suspension of C18-PAF, which is known to form micelle [36], is shown as dotted green lines in Fig. 9.

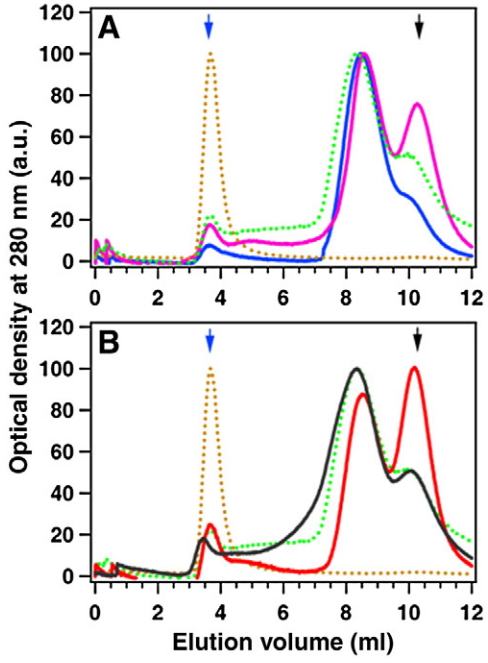

Fig. 9. Size exclusion chromatography of tOx-PL aggregates. An aliquot (100 μl) of tOx-PL suspension was applied to Sepharose 4B column (1.5 × 2.5 cm) and eluted at a flow rate of 0.2 ml/min. Packed column was calibrated by using the following markers: blue dextran for void volume (blue arrows), tryptophan for the total volume (black arrows), aqueous suspension of 50% POPC–50% POPG for the position of MLV (dotted brown lines) and sonicated aqueous suspension of C18-PAF for the elution position of micelle (dotted green lines). Panel A: PazePC (pink line) and PoxnoPC (blue line). Panel B: PGPC (red line) and POVPC (black line).

C18-PAF was always eluted as a major peak at $V_e = 8.16 \pm 0.35$ ml with a small shoulder at 10.13 ± 0.04 ml. Elution profile of aqueous PazePC suspension always gave a major elution peak at 8.48 ± 0.06 (pink line) and a smaller peak at 10.12 ± 0.09 ml, while aggregates of PoxnoPC were eluted as a single major peak at $V_e = 8.47 \pm 0.13$ (blue line). The black lines in panel B represent the elution profile of POVPC which was eluted as a single major peak at 8.38 ± 0.11 ml while PGPC (red line) was always eluted in two peaks, one peak at 8.65 ± 0.14 ml and another at 10.26 ± 0.06 ml. The elution of lipids at $V_e \sim 10.25$ ml, which is the total volume of the column, suggests that some part of lipid molecules remained as monomers and eluted at the total volume of the column. The height of this shoulder/peak was found to differ in different preparations of tOx-PL suspensions. Overall, SEC analysis of four Ox-PLs indicated that they were eluted in the range where C18-PAF micelles was eluted, clearly indicating the micelle or micelle-like particle formation by these tOx-PLs.

3.6. Native PAGE of tOx-PL aggregates

The above results suggest that the aggregates of tOx-PL form micelle or micelle-like particles. Native PAGE analysis is a predominant technique used to determine the molecular size and relative homogeneity of lipoprotein particles [10,21]. Native PAGE analysis of tOx-PL suspension was done to characterize the size of lipid aggregates. In order to detect the aggregates on gel the tOx-PL aggregates were labeled with 0.05 mol% of NBD-DMPG as described under 'Materials and methods'. Trace amount of fluorescent labeled lipid has been used earlier as a marker to track aggregation of lipoprotein complex as well as to detect these particles and it was shown that the trace amount of NBD-DMPG did not affect the aggregation of lipids and lipoproteins particles [21]. In a separate experiment, using SEC of NBD-DMPG (0.05 mol%) labeled and unlabelled aggregates of tOx-PL we also observed that the presence of trace amount of NBD-DMPG does not affect the size of tOx-PL aggregates (data not shown). Suspensions of tOx-PL were subjected to native PAGE analysis on 4–20% gradient gel and after electrophoresis, lipid aggregates and marker protein bands in the gel were visualized as describe under 'Materials and methods'. Representative gel image is shown in Fig. 10 right panel. Aggregates of tOx-PL were observed as a single band (pseudo yellow color) on the gel. Because of their large size, aqueous suspension of 1-myristoyl-2-palmitoyl-*sn*-glycero-3-phosphocholine (MPPC), 1,2-dimyristoyl-*sn*-glycero-3-phosphocholine (DMPC), 1,2-dimyristoyl-*sn*-glycero-3- phosphoglycerol (DMPG), 1-palmitoyl-2-oleoyl-*sn*-glycero-3-phosphocholine (POPC) and 1-palmitoyl-2-oleoyl-*sn*-glycero-3-phosphoglycerol (POPG), prepared similarly as tOx-PL suspension and used as a marker of MLVs, showed bands that

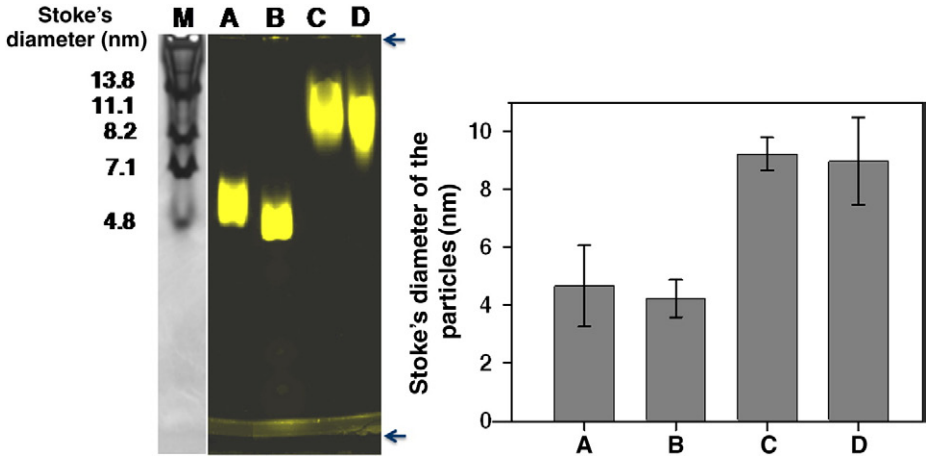

Fig. 10. Native PAGE analysis of tOx-PL aggregates. Aqueous suspension of tOx-PL containing 0.05 mol% NBD-DMPG (used as a fluorescent tracer) was separated on 4–20% gradient tris–glycine gel (Invitrogen). After electrophoresis, gels were directly imaged using a Typhoon Trio™ Variable Mode Imager using excitation wavelength of 488 nm (blue laser) and emission wavelength of 520 nm bandpass 40 filters. The protein (molecular weight marker) bands in the gel were detected by using Bio-Rad Silver Stain Plus kit. Representative gel image is shown in the left panel. Upper and lower arrows in the gel point the bottom of loading wells and dye front, respectively. The Stokes diameter of the tOx-PL aggregates was determined by comparing with the Stokes diameter of protein standards and given in the right panel of the figure. Each data represents the average of six independent experiments and is expressed as mean ± SEM. M; protein molecular weight markers, A; PazePC, B; PGPC, C; PoxnoPC, and D; POVPC.

failed to enter the gel and remained at the bottom of the well (see supplementary data 4). Stokes diameter of tOx-PL aggregates were determined from the calibration curve generated using standard proteins found in the NativeMark protein standards and presented in Fig. 10 right panel. The average Stokes diameter of aggregates of PazePC, PGPC, PoxnoPC and POVPC was found to be 4.23 ± 0.65, 4.66 ± 1.41, 9.22 ± 0.56, and 8.96 ± 1.50, respectively.

3.7. Agarose gel electrophoresis of tOx-PL aggregates

The surface electrostatic properties of tOx-PL aggregates were compared by employing agarose gel electrophoresis. Suspensions of tOx-PL labeled with 0.05% NBD-DMPG was subjected to agarose gel electrophoresis and representative gel image is presented in Fig. 11. Aggregates of tOx-PL were detected as a single band (pseudo yellow color) on the gel. Because of their large size, aqueous suspension of 1-myristoyl-2-palmitoyl-*sn*-glycero-3-phosphocholine (MPPC), 1,2-dimyristoyl-*sn*-glycero-3-phosphocholine (DMPC), 1,2-dimyristoyl-*sn*-glycero-3- phosphoglycerol (DMPG), 1-palmitoyl-2-oleoyl-*sn*-glycero-3-phosphocholine (POPC) and 1-palmitoyl-2-oleoyl-*sn*-glycero-3-phosphoglycerol (POPG), prepared similarly as tOx-PL suspension and used as a markers of MLVs, showed bands that failed to enter the gel and remained at the bottom of the well (see supplementary data 5). Surface potentials (mV) of tOx-PL aggregates were calculated from their electrophoretic velocity using Eqs. (5) and (6) and presented in Fig. 11 right panel. The mean surface potential of aggregates of PazePC and PGPC, which contain truncated *sn*-2 acyl chain bearing carboxyl function, was found to be 15.78 ± 0.78 and 13.99 ± 1.91, respectively. And PoxnoPC and POVPC, which contain truncated *sn*-2 acyl chain bearing aldehydic functional group, possess the surface potential of 3.41 ± 0.38 and 2.92 ± 1.55, respectively.

4. Discussion

All four tOx-PLs used in this study contain 16-carbon, saturated fatty acyl chain (palmitic acid) at the *sn*-1 position and differ only in

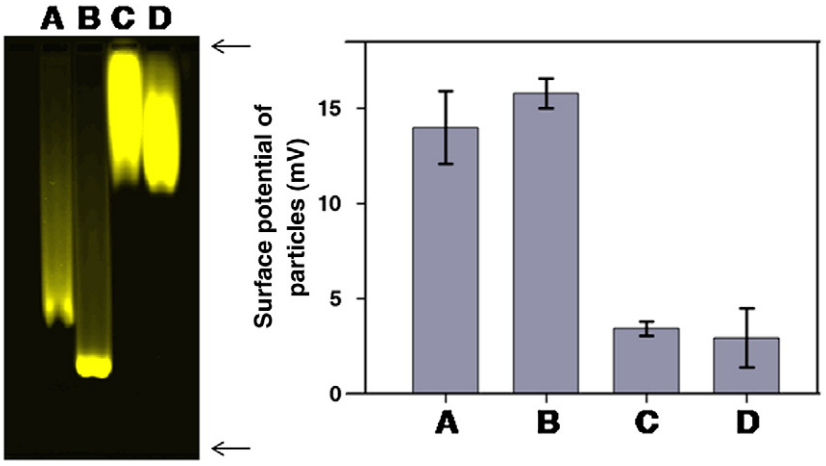

Fig. 11. Agarose gel electrophoresis analysis of tOx-PL aggregates. Aqueous suspension of tOx-PL containing 0.05 mol% NBD-DMPG (used as a fluorescent tracer) was separated on 0.5% agarose gel (10-cm). After electrophoresis, gels were directly imaged using a Typhoon Trio™ Variable Mode Imager using an excitation wavelength of 488 nm (blue laser) and emission wavelength of 520 nm bandpass 40 filters. Representative gel image is shown in the left panel. Upper and lower arrows in the gel point the bottom of loading wells and dye front, respectively. Surface potential of the lipid aggregates was determined using Eqs. (5) and (6) and presented in the right panel of the figure. Each data represents the average of six independent experiments and is expressed as mean ± SEM. M; protein molecular weight markers, A; PazePC, B; PGPC, C; PoxnoPC, and D; POVPC.

the type of oxidatively modified truncated fatty acyl chain at the *sn*-2 position (Fig. 1). PazePC and PGPC contain 9-carbon and 5-carbon fatty acyl chain carrying ω-carboxyl groups, respectively, esterified at the *sn*-2 positions. And PoxnoPC and POVPC contain 9-carbon and 5-carbon fatty acyl chain bearing polar ω-aldehydic groups esterified at the *sn*-2 positions, respectively. In an aqueous solution and at neutral pH, the ω-aldehydic and ω-carboxylic groups are zwitterionic and anionic in nature, respectively. Estimation of CMC of tOx-PLs, using two different fluorescent probes, revealed that the values obtained were in the order POVPC>PGPC>PoxnoPC>PazePC (Table 1). CMC values obtained for PazePC and PoxnoPC in this study are in good agreement with the CMC values previously reported (18.7 and 21.6 μM, respectively) using surface tension measurements [37]. CMC value of monomers in aqueous medium is known to decrease as the acyl chain length of monomer increases. Thus CMC values of tOx-PL bearing truncated *sn*-2 chain of 5-carbons (POVPC and PGPC) are higher than tOx-PL bearing truncated *sn*-2 chain of 9-carbons (PoxnoPC and PazePC).

Characterization of tOx-PL using fluorescent probes revealed that aggregates of individual tOx-PL possess a distinctive set of physicochemical properties. Molecular size determination of aggregates of tOx-PL suggested that the tOx-PL forms micelles in the size range of 4–9 nm. It is important to note here that the size of tOx-PL aggregates was determined by native PAGE analysis by comparing with standard proteins and it may be possible that these standard, soluble proteins marker are not appropriate for calibrating lipid aggregates by native PAGE. In a number of studies, the diameter of smallest, closed vesicles (SUV) was found between 20 and 30 nm [11,14,15], and this diameter range was considered as the minimum diameter allowable for smallest vesicles (SUV) formation and it was proposed that smaller curvature radius would strongly destabilize the closed structure [15]. Thus formation of aggregates of mean diameter 4–9 nm suggests the formation of micelle or micelle-like structure by these four tOx-PLs.

Agarose gel EP of tOx-PL suggests that aggregates of PazePC and PGPC, which contain truncated *sn*-2 acyl chain bearing carboxyl function, has the highest surface potential (net charge) and greatest electrophoretic mobility than aggregates of PoxnoPC and POVPC, which contain truncated *sn*-2 acyl chain bearing aldehydic functional group. It is known that the truncated *sn*-2 acyl chain bearing polar functional group in tOx-PLs adopts extended lipid conformation because of the free energy penalty of keeping a polar group within the hydrophobic milieu of the aggregate [37–39]. Due to this, the polar functional group of the truncated *sn*-2 acyl chain reverses its orientation and reaches the lipid–water interface [39]. The extent of chain reversal of the truncated *sn*-2 acyl chain bearing hydrophilic functional group depends strongly on the length of the fatty acyl chain and the polarity of the functional group it bears. These observations suggest that the physicochemical properties of particular tOx-PL depend on the balance of the size and hydrophobicity of truncated *sn*-2 acyl chain and the hydrophilicity of the polar functional group that is attached to the chain as well as the geometrical characteristics of particular tOx-PL molecules. These features seem to determine the self-association and molecular organization of particular tOx-PL in solution and makes individual tOx-PL assembly unique. It is known that depending upon the packing parameter, the surfactant monomers can self-assemble to form spherical, rod-like micelles, bilayers, vesicles/liposomes, lamellar structures, and so forth in solution [40]. The exact structural characteristics of aggregates of these four tOx-PLs are unknown.

Several reports suggest that different tOx-PLs species exert very different physicochemical effects in lipid membranes and interact differently with proteins and target lipid membranes [2,6–8,39,41–45]. Cationic cytochrome *c* has been shown to bind to micelle of negatively charged PazePC avidly while the interaction with zwitterionic PoxnoPC was weak [42]. In contrast binding of cationic antimicrobial peptides to the PazePC was significantly weaker than to the PoxnoPC [43]. Chain length at the *sn*-2 position has also been correlated with the affinity of apolipoprotein-mimetic peptides suggesting that the type of oxidatively modified acyl chain at *sn*-2 position modulates the biological activities of tOx-PL [44]. Recently Chen et al. [45] has reported the differential effect of tOx-PL species on the properties of isolated mitochondria from Sprague–Dawley rat liver.

Level of tOx-PLs in the plasma represents the risk factor for cardiovascular diseases. Lipoproteins in the plasma are known to bind to tOx-PLs and participate in their transportation [46]. This is proposed to prevent the proinflammatory functions of tOx-PLs and/or enhanced in the degradation of Ox-PLs [46]. Interestingly, apolipoprotein-mimetic peptides have also been shown to exert anti-oxidative and anti-inflammatory properties in animal models [47,48]. Much higher affinity of these mimetic peptides towards the proinflammatory tOx-PLs has been proposed as a mechanism of action of these peptides [47,48]. This high affinity binding enables mimetic peptides to sequester tOx-PLs and prevent their deleterious effects. Additions of apolipoprotein-mimetic peptides have been shown to form nascent discoidal pre-β_1 HDL *in vitro* in human plasma and in mice [49]. Earlier we have observed the preferential binding of lipid binding C-terminal domain of apolipoproteins E and 22-mer peptides derived from this domain to the tOx-PL containing membranes [50]. These protein/peptides also form lipoprotein particles with membrane vesicles containing tOx-PL and the type and amount of tOx-PL present in the lipid vesicles modulate the properties (size, surface charge etc.) of these lipoprotein particles (S. Kar, R.K. Tripathy and A.H. Pande, unpublished data). These observations suggest a plausible correlation between the physicochemical properties of tOx-PLs and their tendency to get sequestered by apolipoproteins/peptides to form lipoprotein particles. It has been proposed that a strategy to design and develop better anti-oxidative and anti-inflammatory peptides should focus on the development of peptides that bind and sequester tOx-PLs with very high affinity [47,48]. Thus it becomes very important that interaction of peptide/protein with specific Ox-PL species should be studied in detail to develop better anti-inflammatory peptides.

In conclusion, we demonstrate that aggregates of four closely related tOx-PLs in aqueous solution possess different physicochemical properties due to difference in their oxidatively modified *sn*-2 acyl chains.

Acknowledgements

This work was supported in partial by the research grants to AHP from NIPER, SAS Nagar (NPLC-AHP and C0410-AHP), Department of Science and Technology (SR/FT/L-93/2006) and Department of Biotechnology (BT/PR9397/BRB/10/554/2007(LETTER I)), New Delhi, Government of India. The authors would like to thank Dr Ipsita Roy, Department of Biotechnology, NIPER, SAS Nagar for allowing the use of Typhoon Imager.

Appendix A. Supplementary data

Supplementary data associated with this article can be found, in the online version, at doi:10.1016/j.bbamem.2009.12.028.

References

[1] A. Catalá, Lipid peroxidation of membrane phospholipids generates hydroxy-alkenals and oxidized phospholipids active in physiological and/or pathological conditions, Chem. Phys. Lipids 157 (2009) 1–11.
[2] G.O. Fruhwirth, A. Loidl, A. Hermetter, Oxidized phospholipids: from molecular properties to disease, Biochim. Biophys. Acta 1772 (2007) 718–736.
[3] H.P. Deigner, A. Hermetter, Oxidized phospholipids: emerging lipid mediators in pathophysiology, Curr. Opin. Lipidol. 19 (2008) 289–294.
[4] G.O. Fruhwirth, A. Hermetter, Mediation of apoptosis by oxidized phospholipids, in: P.J. Quinn, X. Wang (Eds.), Lipids in Health and Disease, Springer, Netherlands, 2000, pp. 351–367.
[5] K. Sabatini, J.P. Mattila, F.M. Megli, P.K.J. Kinnunen, Characterization of two oxidatively modified phospholipids in mixed monolayers with DPPC, Biophys. J. 90 (2006) 4488–4499.

[6] D. Bach, R.F. Epand, R.M. Epand, I.R. Miller, E. Wachtel, The oxidized form of cholesterol 3beta-hydroxy-5-oxo-5, 6-secocholestan-6-al induces structural and thermotropic changes in phospholipid membranes, Chem. Phys. Lipids 161 (2009) 95–102.
[7] M. Valko, D. Leibfritz, J. Moncol, M.T. Cronin, M. Mazur, J. Telser, Free radicals and antioxidants in normal physiological functions and human disease, Int. J. Biochem. Cell Biol. 39 (2007) 44–84.
[8] P. Fu, K.G. Birukov, Oxidized phospholipids in control of inflammation and endothelial barrier, Transl. Res. 153 (2009) 166–176.
[9] C. Reichardt, Solvatochromic dyes as solvent polarity indicators, Chem. Rev. 94 (1994) 2319–2358.
[10] M. Pérusse, A. Pascot, J.-P. Després, C. Couillard, B. Lamarche, A new method for HDL particle sizing by polyacrylamide gradient gel electrophoresis using whole plasma, J. Lipid Res. 42 (2001) 1331–1334.
[11] B.J. Litman, Lipid model membranes. Characterization of mixed phospholipid vesicles, Biochemistry 12 (1973) 2545–2554.
[12] F.M. Megli, L. Russo, E. Conte, Spin labeling EPR studies of the properties of oxidized phospholipid-containing lipid vesicles, Biochim. Biophys. Acta 1788 (2009) 371–379.
[13] D.L. Sparks, M.C. Phillips, Quantitative measurement of lipoprotein surface charge by agarose gel electrophoresis, J. Lipid Res. 33 (1992) 123–130.
[14] M.P. Sheetz, S.I. Chan, Effect of sonication on the structure of lecithin bilayer, Biochemistry 11 (1972) 4573–4581.
[15] C. Huang, J.T. Mason, Geometric packing constraint in egg phosphatidylcholine vesicles, Proc. Natl. Acad. Sci. 75 (1978) 308–310.
[16] E. De Vendittis, G. Palumbo, G. Parlato, V. Bocchini, A fluorimetric method for the estimation of the critical micelle concentration of surfactants, Anal. Biochem. 115 (1981) 278–286.
[17] T. Parasassi, G. De Stasio, G. Ravagnan, R.M. Rusch, E. Gratton, Quantitation of lipid phases in phospholipid vesicles by the generalized polarization of Laurdan fluorescence, Biophys. J. 60 (1991) 179–189.
[18] J.R. Lakowicz, Fluorescence anisotropy, Principles of fluorescence spectroscopy, 3 rd ed., Kluwer Academic/Plenum Publishers, New York, 2006, pp. 353–382.
[19] Y. Asai, T. Nomura, N. Murahashi, K. Iwamoto, Characterization of the physicochemical properties of the micelles of platelet-activating factor (C18:0), Drug Dev. Ind. Pharm. 26 (2000) 671–674.
[20] S.D. Nguyen, D.-E. Sok, Preferable stimulation of PON1 arylesterase activity by phosphatidylcholines with unsaturated acyl chains or oxidized acyl chains at sn-2 position, Biochim. Biophy. Acta 1758 (2006) 499–508.
[21] B.A. Chromy, E. Arroyo, C.D. Blanchette, G. Bench, H. Benner, J.A. Cappuccio, M.A. Coleman, P.T. Henderson, A.K. Hinz, E.A. Kuhn, J.B. Pesavento, B.W. Segelke, T.A. Sulchek, T. Tarasow, V.L. Walsworth, P.D. Hoeprich, Different apolipoproteins impact nanolipoprotein particle formation, J. Am. Chem. Soc. 129 (2007) 14348–14354.
[22] A. Alonso, R. Sáez, F.M. Goñi, The interaction of detergents with phospholipid vesicles: a spectrofluorimetric study, FEBS Lett. 11 (1982) 141–145.
[23] C.C. De Vequi-Suplicy, C.R. Benatti, M.T. Lamy, Laurdan in fluid bilayers: position and structural sensitivity, J. Fluoresc. 16 (2006) 431–439.
[24] B.R. Lentz, Use of fluorescent probes to monitor molecular order and motions within liposome bilayers, Chem. Phys. Lipids 64 (1993) 99–116.
[25] P. Greenspan, S.D. Fowler, Spectrofluorometric studies of the lipid probe, Nile red, J. Lipid Res. 26 (1985) 781–789.
[26] H. Fujii, T. Kawai, H. Nishikawa, Determination of pH in reversed micelles, Bull. Chem. Soc. Jpn. 52 (1979) 2051–2055.
[27] E.B. Abuin, E.A. Lissi, A. Aspee, F.D. Gonzalez, J.M. Varas, Fluorescence of 8-anilinonaphthalene-1-sulfonate and properties of sodium dodecyl sulfate micelles in water–urea mixtures, J. Colloid Interface Sci. 186 (1997) 332–338.
[28] J. Slavík, Anilinonaphthalene sulfonate as a probe of membrane composition and function, Biochim. Biophys. Acta 694 (1982) 1–25.
[29] M. Paternostre, O. Meyer, C. Grabielle-Madelmont, S. Lesieur, M. Ghanam, M. Ollivon, Partition coefficient of a surfactant between aggregates and solution: application to the micelle-vesicle transition of egg phosphatidylcholine and octyl beta-D-glucopyranoside, Biophys. J. 69 (1995) 2476–2488.
[30] E.K. Krasnowska, E. Gratton, T. Parasassi, Prodan as a membrane surface fluorescence probe: partitioning between water and phospholipid phases, Biophys. J. 74 (1998) 1984–1993.
[31] T. Parasassi, E.K. Krasnowska, L. Bagatolli, E. Gratton, Laurdan and Prodan as polarity-sensitive fluorescent membrane probes, J. Fluoresc. 8 (1998) 365–373.
[32] M. Shinitzky, Y. Barenholz, Fluidity parameters of lipid regions determined by fluorescence polarization, Biochim. Biophys. Acta 515 (1978) 367–394.
[33] T. Nomura, Y. Asai, N. Murahashi, K. Iwamoto, Formation of spherical micelles by the novel platelet activating factor receptor antagonist, E5880, Chem. Pharm. Bull. (Tokyo) 48 (2000) 947–950.
[34] X. Zhang, J.K. Jackson, H.M. Burt, Determination of surfactant critical micelle concentration by a novel fluorescence depolarization technique, J. Biochem. Biophys. Methods 31 (1996) 145–150.
[35] S. Lesieur, C. Grabielle-Madelmont, M. Patemostre, M. Ollivon, Size analysis and stability study of lipid vesicles by high performance gel exclusion chromatography, turbidity, and dynamic light scattering, Anal. Biochem. 192 (1991) 334–343.
[36] C. Huang, J.T. Mason, F.A. Stephenson, I.W. Levin, Polymorphic phase behavior of platelet-activating factor, Biophys J. 49 (1986) 587–595.
[37] J.P. Mattila, K. Sabatini, P.K.J. Kinnunen, Oxidized phospholipids as potential novel drug targets, Biophys. J. 93 (2007) 3105–3112.
[38] M.E. Greenberg, X.M. Li, B.G. Gugiu, X. Gu, J. Qin, R.G. Salomon, S.L. Hazen, The lipid whisker model of the structure of oxidized cell membranes, J. Biol. Chem. 283 (2008) 2385–2396.
[39] H. Khandelia, O.G. Mouritsen, Lipid gymnastics: evidence of complete acyl chain reversal in oxidized phospholipids from molecular simulations, Biophys. J. 96 (2009) 2734–2743.
[40] J.N. Israelachvili, Intermolecular and Surface Forces: With Application to Colloidal and Biological Systems, Academic Press, London, 1985.
[41] F.M. Megli, L. Russo, Different oxidized phospholipid molecules unequally affect bilayer packing, Biochim. Biophys. Acta. 1778 (2008) 143–152.
[42] J.P. Mattila, K. Sabatini, P.K. Kinnunen, Interaction of cytochrome c with 1-palmitoyl-2-azelaoyl-sn-glycero-3-phosphocholine: evidence for acyl chain reversal, Langmuir 24 (2008) 4157–4160.
[43] J.P. Mattila, K. Sabatini, P.K. Kinnunen, Oxidized phospholipids as potential molecular targets for antimicrobial peptides, Biochim. Biophys. Acta. 1778 (2008) 2041–2050.
[44] R.F. Epand, V.K. Mishra, M.N. Palgunachari, G.M. Anantharamaiah, R.M. Epand, Anti-inflammatory peptides grab on to the whiskers of atherogenic oxidized lipids, Biochim. Biophys. Acta 1788 (2009) 1967–1975.
[45] R. Chen, L. Yang, T.M. McIntyre, Cytotoxic phospholipid oxidation products. Cell death from mitochondrial damage and the intrinsic caspase cascade, J. Biol. Chem. 282 (2007) 24842–24850.
[46] C. Bergmark, A. Dewan, A. Orsoni, E. Merki, E.R. Miller, M.J. Shin, C.J. Binder, S. Hörkkö, R.M. Krauss, M.J. Chapman, J.L. Witztum, S. Tsimikas, A novel function of lipoprotein [a] as a preferential carrier of oxidized phospholipids in human plasma, J. Lipid Res. 49 (2008) 2230–2239.
[47] B.J. van Lenten, A.C. Wagner, G.M. Anantharamaiah, M. Navab, S.T. Reddy, G.M. Buga, A.M. Fogelman, Apolipoprotein A-I mimetic peptides, Curr. Atheroscler. Rep. 11 (2009) 52–57.
[48] B.J. van Lenten, A.C. Wagner, C.L. Jung, P. Ruchala, A.J. Waring, R.I. Lehrer, A.D. Watson, S. Hama, M. Navab, G.M. Anantharamaiah, A.M. Fogelman, Anti-inflammatory apoA-I-mimetic peptides bind oxidized lipids with much higher affinity than human apoA-I, J. Lipid Res. 49 (2008) 2302–2311.
[49] J.S. Troutt, W.E. Alborn, M.K. Mosior, J. Dai, A.T. Murphy, T.P. Beyer, Y. Zhang, G. Cao, R.J. Konrad, An apolipoprotein A-I mimetic dose dependently increases the formation of preb1 HDL in human plasma, J. Lipid Res. 49 (2008) 581–587.
[50] A.H. Pande, R.K. Tripathy, Preferential binding of apolipoprotein E derived peptides with oxidized phospholipid, Biochem. Biophys. Res. Commun. 380 (2009) 71–75.
[51] http://virtual.yosemite.cc.ca.us/smurov/orgsoltab.htm (Accessed on 8th Dec, 2009).